Reinhold Koch
Thorsten Hesjedal
Klaus Ploog

High-Frequency Acoustic Wave Fields under the Microscope

Nanoacoustics deals with the study of propagation, scattering, diffraction and localization phenomena of acoustic waves on the nanometer length scale, providing important information for the operation of technologically relevant high-frequency filter devices employed, e.g., in mobile phones. Even visualization of the elementary motion of the crystal lattice on an atomic scale has recently become possible. Moreover, since the elastic material properties are accessible to ultrasound, novel nanoacoustics techniques provide a means to study the elastic properties of nanoscopic materials as well as the interplay of elastic phenomena with optical and electronic properties.

Acoustic waves propagating along the surface of a solid, so-called surface acoustic waves (SAWs), are attracting great interest in many respects:

- SAWs are a well-established probe in materials science [1] for quantitative determination of the elastic constants of bulk crystals and thin films [2].
- SAWs play a key role for frequency filtering in mobile phone and satellite telecommunication.
- SAWs are employed in basic studies, e.g., to modify the electronic properties and to induce spin transport in semiconductors [3].

Thus, understanding the interaction of acoustic wave fields with structural features and local elasticity is of great importance for nanoscale determination of elastic constants as well as for the advancement of SAW devices.

Over the last years a variety of different scanning probe techniques has been developed at the Paul-Drude-Institute for the investigation of SAW-related phenomena with nanometer lateral resolution – among them SAW-STM (scanning tunneling microscopy) [4] and SAW-AFM (atomic force microscopy) [5]. They are capable of measuring the SAW amplitude and phase velocity with submicron resolution [6]. The key to the detection of the surface motion at the pace of radio frequency (RF) signals is the non-linear detection characteristics, i.e. the nonlinear dependence of either force or tunneling current on the separation between the probe tip and the sample.

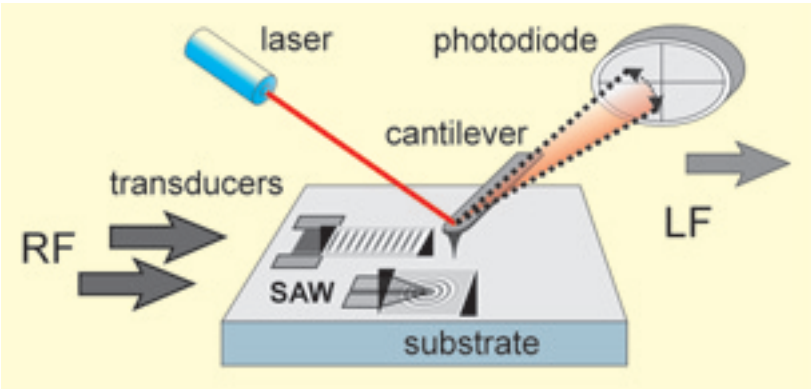

Fig. 1
Experimental setup for SAW scattering experiments with the SAW-AFM.

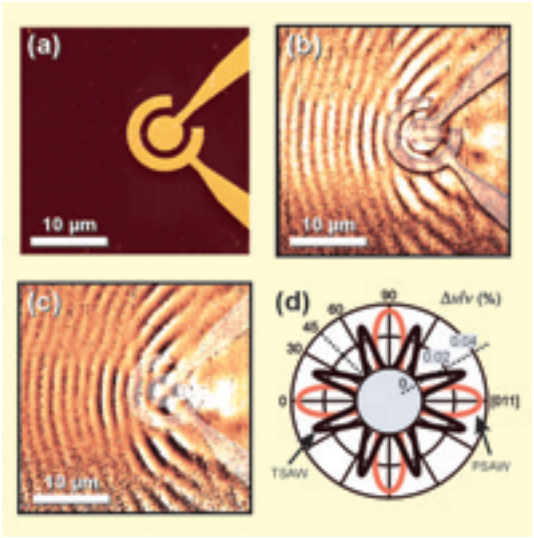

Fig. 2
Point-source excitation investigated by SAW-AFM: (a) Topography of the circular Al transducer structure on GaAs(001) (inner diameter: 4 µm, gap width: 1 µm). The plane sample wave was launched from the left at 890 MHz (λ = 3.2 µm). The circular hot electrode is surrounded by a grounded ring electrode. (b) The amplitude image reveals that directions parallel to and 90° off the reference plane wave propagation direction are preferred wave excitation directions. These are the crystalline directions showing the highest electro-mechanical coupling. (c) The phase image shows periodic phase discontinuities at 0°, which are at half the reference SAW wavelength (λ/2 = 1.6 µm). At 90°, corresponding wave components from the single source and the reference beam interfere, giving the 45° tilted wave fronts. (d) Polar plot of the electro-mechanical coupling coefficient for two surface guided modes: the true SAW (TSAW) and the pseudo SAW (PSAW). In the 0° direction the PSAW converts into a Rayleigh-type SAW and shows high coupling. At 23° the TSAW has its coupling maximum.

SAW-AFM

The AFM probes the surface with a sharp tip mounted on a micrometer-size cantilever, which bends due to forces between the tip and the sample. The cantilever deflection is typically measured with sub-nanometer resolution by an optical detection scheme. The slow response of the cantilever (typical resonance frequencies lie in the 100 kHz range) does not allow a direct detection of very high frequency surface oscillations of SAWs lying in the upper MHz to GHz range. We succeeded to detect RF surface oscillations by a more sophisticated approach, where – similar to a crystal radio detector – the non-linear force-distance relationship is utilized for the demodulation of high-frequency signals. This method resembles a mechanical diode and delivers a signal that is proportional to the wave amplitude [7]. The experimental setup of a SAW-AFM is illustrated in Fig. 1 [5, 6]. For the phase measurement, the introduction of two RF fields at slightly detuned frequencies to the mechanical diode results in oscillation signals at their difference frequency (chosen to be below the cantilever's resonance frequency). The SAW-related amplitude and phase signals are detected by a lock-in amplifier. A similar nonlinear coupling mechanism also exists for purely transverse oscillations leading to cantilever torsions [7].

Crystal Anisotropy in Point-Source Excitation

The study of elementary wave phenomena, like scattering from a single dot or the wave excitation by single sources, is extremely challenging, as the involved amplitudes are well below 1 Å. The experimental trick to measure these small oscillations is to insonify the structure of interest by a well-defined plane wave. This additional oscillation of larger amplitude is detuned in frequency with respect to the waves under investigation. Again, the signal at the difference frequency is a result of the mixing at the *mechanical diode*. The experimental results demonstrate the very high vertical resolution of the SAW-AFM, which is smaller than 0.01 pm, in combination with nm lateral resolution [8]. Mapping of the wave field of single sources opens up new ways for the modeling and improvement of acoustic devices that is based on detailed measurements instead of empirical models.

Fig. 2 shows the excitation characteristics of a single acoustic source. In particular, waves were found that are excited perpendicular to the main excitation direction. For technolgical applications this means that waves are leaking out of the device structure, thus limiting its performance. The circular source delivers the most complex and informative phase and amplitude pattern. The topography in Fig. 2a shows the circular center electrode, surrounded by a ring electrode. The amplitude (Fig. 2b) and phase images (Fig. 2c) show that most of the energy is radiated in a cruciform pattern defined by the crystalline symmetry. From this measurement, two important properties of the piezoelectric material can be extracted: (i) the crystalline directions under which waves are excitable can be determined, (ii) the efficiency of their excitation by means of interdigital transducers can be measured locally. For comparison, Fig. 2d shows the polar plot of the respective electro-mechanical coupling coefficient – an important characteristic of SAW applications – for the two SAW modes calculated by a transfer matrix method. It reproduces nicely the cruciform radiation pattern observed in the experimental amplitude and phase images.

Nanoakustik

Akustische Oberflächenwellen (SAW) spielen eine entscheidende Rolle für die Frequenzfilterung in der Mobiltelefon- und Satellitenkommunikation. Am PDI wurden eine Reihe von Rastersondenmethoden entwickelt, mit denen die Ausbreitung, Brechung und Beugung hochfrequenter akustischer Wellenfelder mit einer Ortsauflösung im Nanometerbereich untersucht werden können. Diese neuen Methoden liefern damit wichtige Informationen, insbesondere für die hochaktuelle Entwicklung von GHz-Filterelementen. Kürzlich ist es gelungen, die elliptische Trajektorie der Bewegung der Oberflächenatome anhand eines Flächenelementes von nur 3x3 nm^2 zu bestimmen, was nun auch Untersuchungen der elastischen Eigenschaften auf der Nanometerskala in Aussicht stellt.

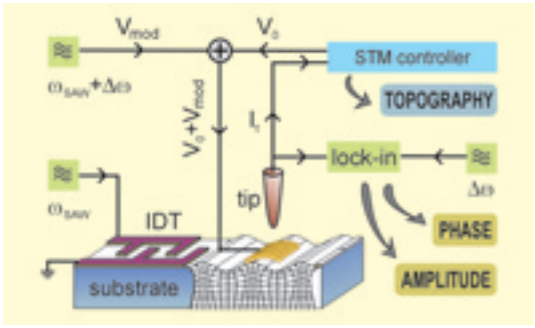

Fig. 3
Experimental setup of a SAW-STM.

SAW-STM

The experimental setup of a SAW-STM is schematically illustrated in Fig. 3. The STM tip is positioned above the conducting film on the piezoelectric sample, which is located in the propagation path of the SAW excited by the transducer on the left. The SAW-induced surface oscillations at the frequency ω_{SAW} give rise to a RF contribution to the tunneling current between tip and conducting layer. The RF component is mixed at the non-linear current-distance characteristics of the tunneling gap with a RF voltage V_{mod} at the frequency $\omega_{SAW} + \Delta\omega$, which is added to the common DC tunneling voltage V_0. Conveniently, the mixing signal at the difference frequency $\Delta\omega$ is laid into the higher kHz range, which is easily accessible for lock-in detection, but exceeds significantly the bandwidth of the STM feedback. The mixing signal, which is recorded simultaneously with the topography, exhibits the amplitude and phase information of the SAW and is suitable to study the influence of local inhomogeneities on the wave propagation with a lateral resolution which is much smaller than the acoustic wavelength.

Nanoscale Imaging of Longitudinal SAWs

With our ultrahigh vacuum SAW-STM we investigated the propagation of high-velocity pseudo-SAWs (HVP-SAWs) on Y-cut $LiNbO_3$. PSAWs are special types of PSAWs which are known for leaking energy into the bulk during propagation. Since HVPSAWs exhibit much higher phase velocities than normal SAW modes, the operating frequency of SAW devices can be increased without necessarily decreasing the lithographical fea-

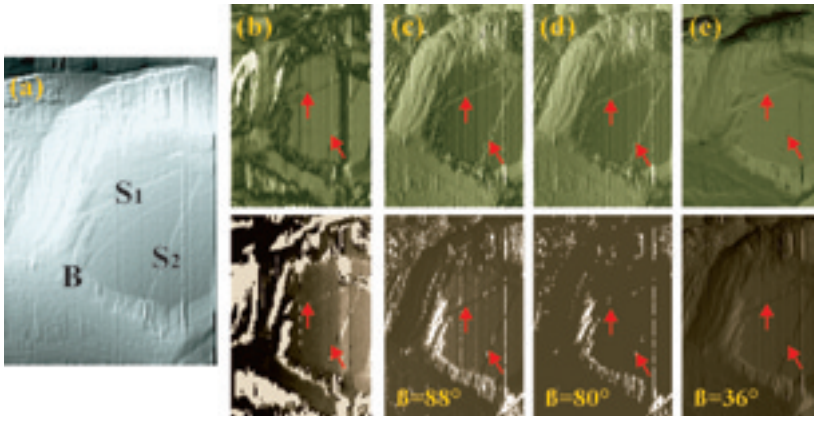

Fig. 4
(a) 62 x 42 nm² topview of a 100 nm thick Au film on Y-cut $LiNbO_3$ as well as (b) amplitude (top) and phase images (bottom) of a HVP-SAW, all recorded simultaneously with the SAW-STM. (c) – (e) Simulated amplitude (top) and phase images (bottom) at different angles β of the oscillation ellipse. The best agreement with experiment is achieved with β = 88°.

ture sizes. Compared with the well known Rayleigh waves, HVSAWs have a predominant longitudinal oscillation behavior. They are easily excited, e.g., on Y-cut $LiNbO_3$, where the component perpendicular to the surface amounts only 3% of the longitudinal component within the surface (compared to 130% in the case of the corresponding Rayleigh wave). Although HVPSAWs have been extensively studied theoretically in the past, very little experimental work has been devoted to them because of the difficulties involved in detecting their predominant in-plane polarized oscillation with other techniques (e.g., optical methods).

Fig. 4a shows an STM topview of the conducting Au layer [9]. The film exhibits a textured morphology and consists of crystalline islands with mainly hexagonal and occasionally rectangular shapes and dimensions ranging from 10 to 150 nm. In Fig. 4a a grain with a 30-nm-wide horizontal plateau is depicted that is framed by a 2-nm-high bulged border (B). The plateau consists of atomically flat extended (111) terraces separated by two

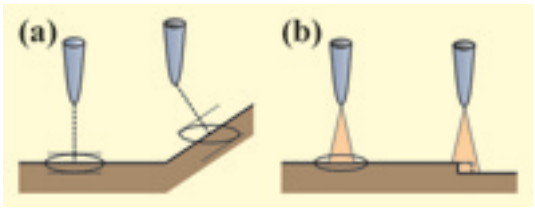

Fig. 5
Schematic illustration of the SAW detection by an SAW-STM: (a) on facets that are larger than the tunneling cone, and (b) at an atomic step which lies inside the (shaded) tunneling cone.

monosteps, S_1 and S_2. Amplitude and phase at the difference frequency, which were simultaneously extracted from the tunneling current while scanning the topography, are displayed in Fig. 4b. They impressively demonstrate that SAW-STM is indeed sensitive to SAWs with negligible out-of-plane oscillation. Interestingly, many details of the surface morphology can also be recognized in the two SAW-induced images, such as the plateau with two monosteps on its bulged border.

When a SAW is excited, each surface element follows an elliptical trajectory given by the longitudinal and perpendicular ellipse axes u_1 and u_3, respectively. Since the electrons tunnel mainly along the shortest line between tip apex and sample surface, in SAW-STM experiments on corrugated surfaces, the geometrical projection of the oscillation ellipse is monitored by the STM tip (*cf.* Fig. 5a). Accordingly, amplitude A and phase φ of the mixing signal depend on the local inclination of the surface with respect to the propagation direction of the SAW, as well as on its eccentricity $\beta = \arctan(u_1/u_3)$. By introducing spherical coordinates with respective polar and azimuthal angles Θ and Φ one obtains [10]:

$$A \propto u_0 \sqrt{\sin^2\beta\cos^2\Phi\sin^2\Theta + \cos^2\beta\cos^2\Theta}$$

$$\varphi = \arctan(\tan\beta\cos\Phi\tan\Theta)$$

Whereas on top of a flat horizontal terrace (Θ = 0°) only the normal component ($u_3 = u_0 \cos\beta$) of the oscillation trajectory is measured, the in-plane component ($u_1 = u_0 \sin\beta$) is additionally contributing at inclined facets. Note that the tip delay at one data point is about 2 ms. Therefore the tunneling current averages over about 400,000 oscillation cycles and amplitude and phase images are uniform within terraces. Due to the small length scale of typical STM images compared with the SAW wave-length (3.5 μm) the relative phase shift induced by the linear SAW phase delay with increasing distance from the IDT is about 4° for the entire image of Fig. 4a.

The comparison of the experimental results with amplitude and phase images simulated by employing the two equations given above enables the quantitative determination of the eccentricity β of the SAW oscillation ellipse. Figures 4c e show simulations for different values of β using the experimental topography of Fig. 4a as an input parameter. Obviously, the best agreement with the experiment is achieved for β close to the theoretical value of HVP-SAWs on Y-cut $LiNbO_3$, namely $\beta_{th} = 88°$. For β = 80° the agreement with the experiment is significantly decreased, allowing to estimate the experimental accuracy to ±5°. Note that the respective amplitude contrast is even inversed for β = 36°, i.e. the value of the Rayleigh wave (Fig. 4e). The smallest partial scanned area to measure quantitatively the eccentricity of the oscillation ellipse due to the SAW-induced surface motion is as small as 3 x 3 nm². These promising results therefore demonstrate that the SAW-STM method presented here is suited to measure elastic constants on a nanometer scale.

Whereas the influence of topography is reproduced on a quantitative level for structural features with dimensions above 1–2 nm, a different situation is encountered when the feature of interest lies inside the tunneling regime. Fig. 5b compares tunneling from a horizontal terrace and close to a step edge. As long as the tip scans the terrace (Fig. 5b, left), mainly the vertical oscillation component is detected; the in-plane oscillation of the SAW is not accompanied by a change of the overall tunneling current. At a step (Fig. 5b, right) the upper terrace dominates the tunneling current due to the exponential decay with distance. Due to

the SAW-induced lateral motion of the step edge the area of the upper terrace underneath the STM tip varies periodically, which leads to a component proportional to $u_1 \sin(\omega t)$ in the tunneling current; note that its phase is shifted by $\pi/2$ with respect to the vertical component. A detailed analysis reveals that also the mixing signal measured at a step edge contains information about the eccentricity, and thus of the ratio u_1/u_3 of the surface oscillation. These findings are indeed encouraging as quantitative information on the SAWs can be deduced not only from highly corrugated morphologies but also from nanoscale features present on flat surfaces.

Outlook

The RF scanning probe techniques developed at the PDI have proven to be powerful methods to study SAWs on a nanoscopic length scale. The new techniques are sensitive to both the transversal and longitudinal oscillation components of the SAW and are therefore well suited to identify and investigate the propagation of SAWs with even negligible out-of-plane oscillation. In particular, the local measurements of the phase, and thus the phase velocity, by SAW-AFM as well as of the eccentricity of the oscillation ellipse by SAW-STM are very promising for future studies of nanoscale elasticity. Since both properties are directly related to the elastic constants, the local elastic properties at grain boundaries, dislocations and other crystal defects eventually come within reach.

References

[1] *Hess, P.:* Physics Today 55, 42 (2002).
[2] *Royer, D./Dieulesaint, E.:* Elastic Waves in Solids I, Springer-Verlag, Berlin 2000.
[3] *Sogowa,T. /Santos, P./Zhang, S. K./Eshlagi, S./Wieck, A. D./Ploog, K. H.:* Phys. Rev. Lett. 87, 276601 (2001).
[4] *Chilla, E./Rohrbeck, W./Fröhlich, H.-J./Koch, R./Rieder,K. H.:* Appl. Phys. Lett. 61, 3107 (1992).
[5] *Hesjedal,T./Chilla, E./Fröhlich, H.-J.:* Appl. Phys. A 61, 237 (1995).
[6] *Chilla, E./Hesjedal, T./Fröhlich, H.-J.:* Phys. Rev. B Vol. 55 (1997), p. 15852.
[7] *Behme, G./Hesjedal, T./Chilla, E./Fröhlich, H.-J.:* Appl. Phys. Lett. 73, 882 (1998).
[8] *Hesjedal, T./Behme, G.:* Europhys. Lett. 54, 154 (2001).
[9] *Yang, J./Voigt, P. U./Koch, R.:* Appl. Phys. Lett. 82, 1866 (2003).
[10] *Chilla, E./Rohrbeck, W./Fröhlich, H.-J./Koch, R./Rieder, K. H.:* Ann. Phys. 3, 21 (1994).

Coworkers
G. Behme, E. Chilla, P. U. Voigt, J. Yang

PD Dr. Reinhold Koch

Born 1954. Studies of Chemistry in Innsbruck, Austria, PhD in Physical Chemistry 1982. Postdoc stays at the Stanford/NASA Joint Institute for Surface and Microstructure Research, USA (Max-Kade-Followship), and at the University of Innsbruck. 1988–1998 Assistent teacher at the Institute of Experimental Physics of the Free University Berlin, 1993 Habilitation. 1998 Paul Drude-Institute for Solid State Electronics, since 1999 Leader of the Nanoacoustics group. Karl-Scheel-Award 1994.

Contact
Paul Drude-Institute for Solid State Electronics
Hausvogteiplatz 5–7
D–10117 Berlin
Phone: +49-30-20377–414
Fax: +49-30-20377–257
E-Mail: koch@pdi-berlin.de
www.pdi-berlin.de/nanoac/nanoac.shtml

Dr. Thorsten Hesjedal

Born 1969. Studies of Physics at the Universities of Stuttgart and Tübingen, PhD in Physics 1997. 1998–2001, Visiting Scholar at Stanford University and collaborations with IBM Almaden and Hewlett Packard in Palo Alto. Carl Ramsauer Award 1998 for his pioneering work on ultrasonic scanning probe microscopy. Since 2002 scientific staff member at the PDI.

Contact
Paul Drude-Institute for Solid State Electronics
Hausvogteiplatz 5–7
D–10117 Berlin
Phone: +49-30-20377–260
Fax: +49-30-20377–257
E-Mail: hesjedal@pdi-berlin.de

Prof. Dr. Klaus Ploog

Born 1941. Studies of Chemistry in Kiel and Munich, PhD in Chemistry 1970. 1991 Professor of Materials Science at Darmstadt University of Technology. 1992 Director of the Paul-Drude-Institute for Solid State Electronics and 1993 Professor of Materials Science at Physics Department of Humboldt-Universität. 1984–2003 Visiting Research Professor at NTT, Tokyo and Atsugi, Mitsubishi Central Research Laboratories, Kyushu Institute of Technology, Tokyo Institute of Technology, Teikyo University, ETSI de Telecomunicacion, UPM, Madrid, Hokkaido University, Sapporo, TU Eindhoven.
Awards: 1983 Technology-Transfer-Award of German Ministry of Research and Technology, 1989 Award of Italian Physical Society, 1990 Philip-Morris-Research Award, 1998 IBERDROLA Ciencia y Technologia Award, 1999 Max Planck Research Award for International Cooperation, 2003 Welker Award.

Contact
Paul Drude-Institute for Solid State Electronics
Hausvogteiplatz 5–7
D–10117 Berlin
Phone: +49-30-20377–352
Fax: +49-30-20377–201
E-Mail: ploog@pdi-berlin.de